Targeted disruption of Rab1a causes early embryonic lethality

YIN WU, DARONG YANG and GUO-YUN CHEN

Children's Foundation Research Institute at Le Bonheur Children's Hospital, Department of Pediatrics, University of Tennessee Health Science Center, Memphis, TN 38103, USA

Received November 15, 2021; Accepted January 19, 2022

DOI: 10.3892/ijmm.2022.5101

Abstract. Guanosine nucleotide diphosphate (GDP) dissociation inhibitor 2 (GDI2) regulates the GDP/guanosine triphosphate (GTP) exchange reaction of Rab proteins by inhibiting the dissociation of GDP and the subsequent binding of GTP. The present study aimed to determine the function of Rab1a *in vivo*, and thus generated mice with a trapped *Rab1a* gene. It was demonstrated that *Rab1a* is essential for embryonic development. It was also found that one functional Rab1a allele was sufficient for development in a heterozygous murine embryo, whereas a double mutant led to embryonic lethality. The dissection of uteri on embryonic day (E)10.5-14.5 yielded no homozygous embryos, indicating that homozygotes die between E10.5 to E11.5. The gene trap construct contains a β-galactosidase/neomycin reporter gene, allowing for heterozygotes to be stained for β-galactosidase to determine the tissue-specific expression of Rab1a. Rab1a was found to be highly expressed in the small intestine of both adult mice and embryos, although its expression levels were low in the brains of embryos. Moreover, there was no significant change in cytokine production and survival in wild-type and heterozygous Rab1a$^{+/-}$ mice following a challenge with lipopolysaccharide. On the whole, the present study demonstrates that the disruption of the *Rab1a* gene causes embryonic lethality and homozygotes die between E10.5 and E11.5, suggesting that *Rab1a* is essential for the early development of mouse embryos.

Introduction

Rab proteins are a subfamily of the Ras superfamily of small GTPases that are key regulators of intracellular membrane trafficking, from the formation of transport vesicles to their fusion with membranes. These proteins can be detected in an inactive or active conformation, depending on the nucleotide-bound status, and are considered switches that cycle between an active, membrane-associated status and an inactive cytosolic status. To date, >70 mammalian Rab proteins have been identified (1). Some Rab proteins exhibit a regulated expression, tissue-specific expression, or developmental-specific expression, while others are ubiquitously expressed (1). Each Rab protein exhibits a characteristic subcellular distribution (2).

Rab1a regulates vesicular protein transport from the endoplasmic reticulum to the Golgi apparatus (3,4) and to the cell surface (5). It also plays a role in secretion of interleukin (IL)-8 and growth hormones. Rab1a function has been implicated in neuronal differentiation (6) and cardiac development (7). The overexpression of Rab1a in transgenic mice has been shown to be associated with an increased cardiac mass and cardiac hypertrophy, leading to cardiomyopathy (7). Rab1a activity is also targeted by bacterial (8-10) and viral pathogens (11). Additionally, Rab1a regulates the mTORC1 pathway in glucose homeostasis (12), colorectal cancer (13), liver cancer development (14) and breast cancer cells (15).

The guanosine nucleotide diphosphate (GDP) dissociation inhibitor (GDI) proteins regulate the Rab family GTPase function by binding to Rab GTPase in its GDP-bound inactive form to retrieve it from the cell membrane and to maintain a soluble pool of inactive proteins ready to be re-used (16). The GDI family includes the GDI1 and GDI2 proteins. GDI1 is expressed primarily in neural and sensory tissues, whereas GDI2 is ubiquitously expressed (17).

In a recent study, it was demonstrated by the authors that GDI2 binds to the immunoreceptor tyrosine-based inhibitory motif (ITIM) domain of sialic acid-binding immunoglobulin-type lectin G (Siglec-G) in hematopoietic cells, such as B-1a cells under conditions of normal homeostasis, whereas Rab1a is recruited to the ITIM domain during bacterial infection (18). Therefore, it was hypothesized that GDI2 and Rab1a may regulate the immune response through interaction with the ITIM domain during bacterial infection. The present study thus aimed to explore the function of Rab1a *in vivo* by generating a *Rab1a* null mutant model with a trapped *Rab1a* gene. The homozygous deletion of the *Rab1a* gene resulted in early embryonic lethality. Rab1a protein was expressed from the trapped gene during early post-implantation development, suggesting a critical role of Rab1a in the transport of materials between organelles in eukaryotic cells.

Correspondence to: Professor Guo-Yun Chen, Children's Foundation Research Institute at Le Bonheur Children's Hospital, Department of Pediatrics, University of Tennessee Health Science Center, 50 N. Dunlap Street, Memphis, TN 38103, USA
E-mail: gchen14@uthsc.edu

Key words: Rab1a, guanosine nucleotide diphosphate dissociation inhibitor 2, embryonic lethality, small intestine, immunoreceptor tyrosine-based inhibitory motif

Materials and methods

Reagents. Rabbit anti-mouse Rab1a antibodies (cat. no. sc-311) were obtained from Santa Cruz Biotechnology, Inc. and lipopolysaccharide (LPS; from *Escherichia coli* (*E. coli) 055:B5* strain] were purchased from MilliporeSigma. Goat anti-mouse β-actin (cat. no. sc-1615) and horseradish peroxidase (HRP)-conjugated goat anti-rabbit IgG antibodies (cat. no. sc-2004) were purchased from Santa Cruz Biotechnology, Inc. 5-Bromo-4-chloro-3-indolyl β-D-galactopyranoside (X-gal) was obtained from Thermo Fisher Scientific, Inc.

Generation of Rab1a mutant mice. A male chimeric mouse generated from the ES cell line, XB498, was obtained from Bay Genomics, LLC. The ES cell line, XB498, was generated by using a gene trap protocol with the trapping construct pGT0pfs containing the intron from the engrailed 2 homeobox gene upstream of the gene encoding the β-galactosidase/neomycin-resistance fusion protein (please see Fig. 1 and https://igtc.org/cgi-bin/annotation.py?cellline=XB498). Genotyping was determined by the polymerase chain reaction (PCR) analysis of DNA from tail biopsies, as previously described (19).

PCR-based genotyping of mice. Aliquots of 0.1 μg (10 μl) DNA were mixed with 10 μl of 2X GoTaq Green Master Mix buffer (Promega Corporation) and 10 pmol of each primer, as previously described (19). PCR amplification was carried out at 96˚C for 2 min, with 35 cycles of 96˚C for 10 sec, 55˚C for 30 sec, and 72˚C for 60 sec. To screen for the homologous recombination of DNA, the following primers were used: P1, 5'-ACTGAGTATCCCTGGCTGGC-3' and P2, 5'-AAGAGT AGGCTAGCCAGTCA-3'. The wild-type (WT) allele was not amplified (no band was detected), while the mutant allele produced a 300-bp band corresponding to the amplification product. The following primers were also used to confirm the presence or absence of the WT allele: P3, 5'-AGCACAGAC AAGCACAGTAG-3' and P4, 5'-GTTATCAGGCTTGGCAGC AG-3'. The amplification of the WT allele produced a 485-bp band, while the mutant allele was not amplified and therefore produced no band. Therefore, WT mice (*Rab1a*$^{+/+}$) produced a WT 485-band and homozygous mice (*Rab1a*$^{-/-}$) produced a 300-bp band, while heterozygous mice (*Rab1a*$^{+/-}$) produced both a WT 485-bp band and a mutant 300-bp band. The PCR products were separated by agarose gel electrophoresis, stained with SYBR® Safe DNA Gel Stain (Thermo Fisher Scientific, Inc.) and visualized using Axygen Gel Documentation System (Corning, Inc.).

X-gal staining of mouse tissue and mouse embryos. The X-gal staining of tissues (frozen sections for E7 and E15 embryos and adult small intestine samples were prepared from WT or *Rab1a*$^{+/-}$ mice) was performed using standard procedures, as previously described (20). Embryos were embedded in optimal cutting temperature (OCT) compound and subjected to cryo-sectioning to generate slices that were 8-μm-thick. The cryosections were fixed in X-gal fixation buffer (0.1 M phosphate buffer, pH 7.3, 5 mM EGTA, 2 mM $MgCl_2$, 0.2% glutaraldehyde) for 15 min, washed three times with X-gal wash buffer (0.1 M phosphate buffer, pH 7.3, 2 mM $MgCl_2$), and stained overnight at 37˚C in X-gal staining buffer [0.1 M phosphate buffer, pH 7.3, 2 mM $MgCl_2$, 5 mM $K_4Fe(CN)_6$, $3H_2O$, 5 mM $K_3Fe(CN)_6$, 1 mg/ml X-gal]. The stained sections were washed three times with X-gal wash buffer and mounted in Aquatex® aqueous mounting medium (MilliporeSigma). Images were acquired using an EVOS FL Auto Imaging System (Thermo Fisher Scientific, Inc.).

Experimental animal models. The *Rab1a* mutant male mouse was from the Mutant Mouse Regional Resource Center (MMRRC) at the University of California, Davis (UC Davis). For backcrossing, two WT C57BL/6 female were obtained from Jackson Laboratory. A total of 159 (male, 53; female, 106) adult mice (*Rab1a*$^{+/+}$, 16; *Rab1a*$^{+/-}$, 16 for LPS treatment experiments and *Rab1a*$^{+/-}$, 127 for producing pups and embryos) (6-8 weeks of age; weight, 20-25 g), as well as 250 pups and 77 embryos were produced in the laboratory of Dr GYC and used in the present study. The mice were maintained in individually ventilated cages (25˚C and 55-65% humidity) with a 12/12-h light/dark cycle and free access to standard laboratory mouse chow and water. Age- and sex-matched WT littermates were used as controls for heterozygous *Rab1a*$^{+/-}$ or homozygous *Rab1a*$^{-/-}$ mice. All procedures involving animals were approved by the University of Tennessee Health Science Center (UTHSC) Animal Care and Use Committee (IACUC), protocol nos. 17-117 (approved January 29, 2018) and 20-0211 (approved January 26, 2021). At the end of each experiment, adults and neonates >10 days of age were euthanized with CO_2 followed by cervical dislocation. The CO_2 displacement rate for a euthanasia chamber is 30-70% per min (as a percentage of the chamber volume per minute). To assess the period of developmental failure, pregnant mice were euthanized with CO_2 followed by cervical dislocation and embryos from heterozygote hybridization were collected on embryonic day (E)10.5, E11.5, E12.5 and E14.5, and genotyped using PCR as stated above. Neonates <10 days of age were euthanized with 5% isoflurane followed by decapitation with scissors. For the mouse model of endotoxemia, age, sex and weight-matched WT and *Rab1a*$^{+/-}$ mice were injected (i.p.) with 10 mg/kg LPS in PBS. The mice were monitored for up to 5 days.

Western blot analysis. Embryo lysates were prepared by incubation in lysis buffer (20 mM Tris-HCl, 150 mM NaCl, 1% Triton X-100, pH 7.6, including protease inhibitors, 1 μg/ml leupeptin, 1 μg/ml aprotinin and 1 mM phenylmethylsulfonyl fluoride), sonication, centrifugation was performed at 4˚C and at 16,200 x g for 5 min to remove cell debris. Proteins in the lysates were determined by BCA and separated on 10% SDS-PAGE gels, transferred to PVDF membranes, and then examined by western blotting, as previously described (21). After blocking with 5% skimmed milk in PBS-T (PBS with 0.01% Tween-20) at room temperature for 1 h, the blots were incubated with goat anti-mouse β-actin primary antibodies (1:1,000 dilution) at 4˚C overnight. The membranes were then incubated with horseradish peroxidase (HRP)-conjugated goat anti-rabbit IgG secondary antibodies (1:5,000 dilution) at room temperature for 2 h and the signal was detected using a luminol-based enhanced chemiluminescence (ECL) kit (Santa Cruz Biotechnology, Inc.).

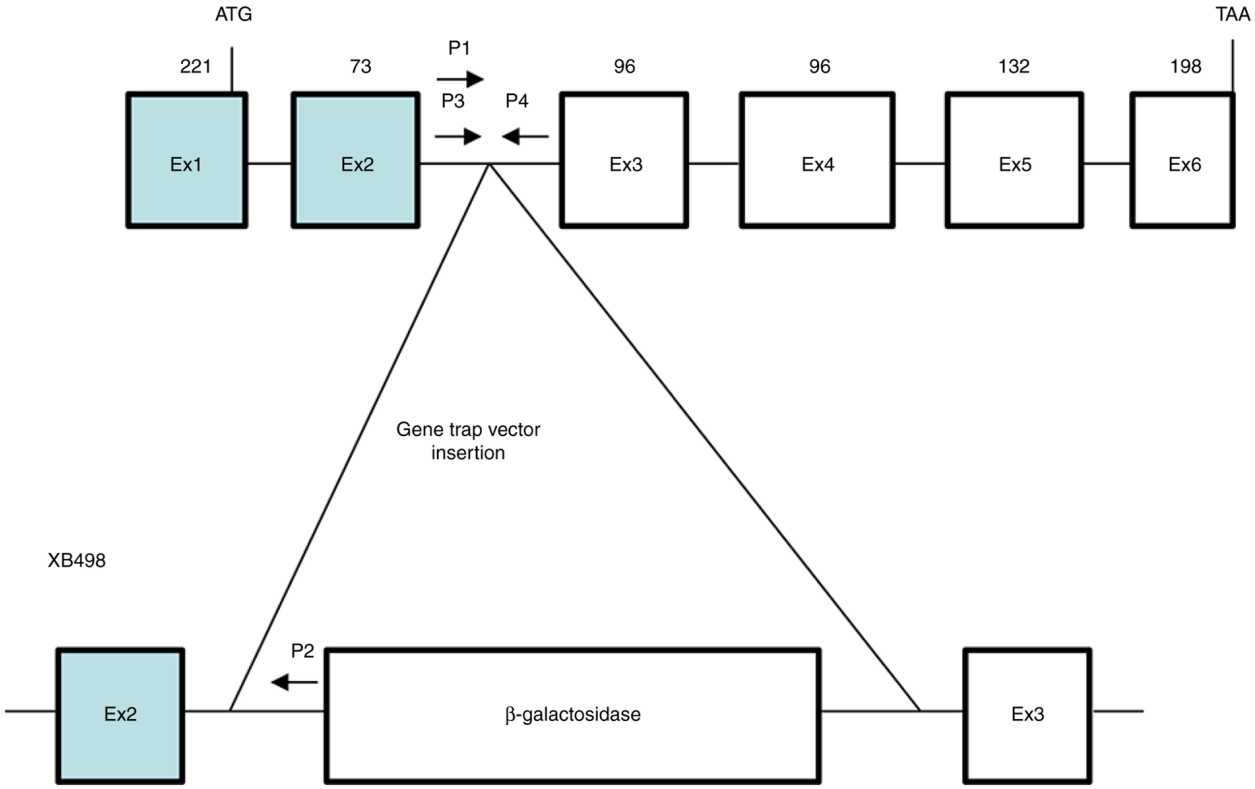

Figure 1. Localization of the gene trap vector interrupting the *Rab1a* gene. Genomic exon organization of the murine *Rab1a* gene. The numbers above the exons correspond to the *Rab1a* cDNA. The second row presents a diagram of the mutated allele of *Rab1a* gene in which a β-galactosidase gene was inserted between exons 2 and 3. The four primers (P1, P2, P3 and P4) used for genotyping are shown. Ex, exon.

Histological analysis and immunohistochemistry. Tissues from WT or mutant mice were fixed in 4% paraformaldehyde at room temperature for 24 h, dehydrated and embedded in paraffin according to the standard procedure and as previously described (19). Sections at a thickness of 5 μm were cut, dewaxed in xylene, dehydrated in 100% ethanol and then stained with hematoxylin and eosin [H&E; hematoxylin (cat. no. SH26-500D, Fisher Chemical; Thermo Fisher Scientific, Inc.) for 3 min and eosin (cat. no. S176-16OZ, Poly Scientific R&D Corp.) for 30 sec] at room temperature or reacted with anti-mouse Rab1a antibody (1:1,000; cat. no. sc-311, Santa Cruz Biotechnology, Inc.) at room temperature for 1 h. The sections were washed in phosphate-buffered saline (PBS) and subsequently incubated with HRP-conjugated goat anti-rabbit secondary antibodies (1:1,000; cat. no. sc-2004, Santa Cruz Biotechnology, Inc.) at room temperature for 30 min. After being washed in PBS, slides were developed with 3,3'-diaminobenzidine (DAB) and counterstained with hematoxylin for 10 sec at room temperature. For the control, immunohistochemical staining was performed by omitting the primary antibody. No significant staining was observed upon control staining (data not shown). Images were acquired using an EVOS FL Auto Imaging System (Thermo Fisher Scientific, Inc.).

Measurement of inflammatory cytokine levels. Blood samples were obtained at the indicated time points and cytokines in the serum and measured using a mouse cytokine bead array designed for inflammatory cytokines (cat. no. 552364; BD Biosciences), as previously described (21-24). The kit quantitatively detects the levels of the cytokines, IL-6, IL-10, monocyte chemoattractant protein-1 (MCP-1), interferon-γ (IFN-γ), tumor necrosis factor (TNF) and the IL-12 heterodimer (IL-12p70).

Statistical analysis. The differences in cytokine concentrations were analyzed using two-tailed t-tests in single pairwise comparisons calculated with Excel (Microsoft). Data are presented as the mean ± SD. A value of $P<0.05$ was considered to indicate a statistically significant difference.

Results

Generation of Rab1a mutant mice. To determine the function of Rab1a *in vivo*, we obtained a *Rab1a* mutant mouse from MMRRC which was generated by the blastocyst injection of a *Rab1a* trapped embryonic stem cell clone (XB498, Bay Genomics). Gene disruption was caused by the insertion of the retroviral gene trap vector pGT0pfs containing a promoterless β-galactosidase reporter gene. Selection for the expression of the gene requires transcription from an endogenous cellular promoter and consequently, a mutation in a cellular gene. The expression of the tagged gene can be examined by staining for β-galactosidase. The methods used for gene trap mutagenesis have been previously reported (25-27). In the XB498 ES cell line, the gene trap vector pGT0pfs was inserted between exons 2 and 3 of *Rab1a* (Fig. 1 and Data S1); the point of insertion was confirmed by PCR and DNA sequencing (Fig. 2 and Data S2). Offspring were genotyped by PCR analyses using primers P1 and P2 for the knockout (KO) PCR and primers P3 and P4 for the WT PCR (Fig. 1).

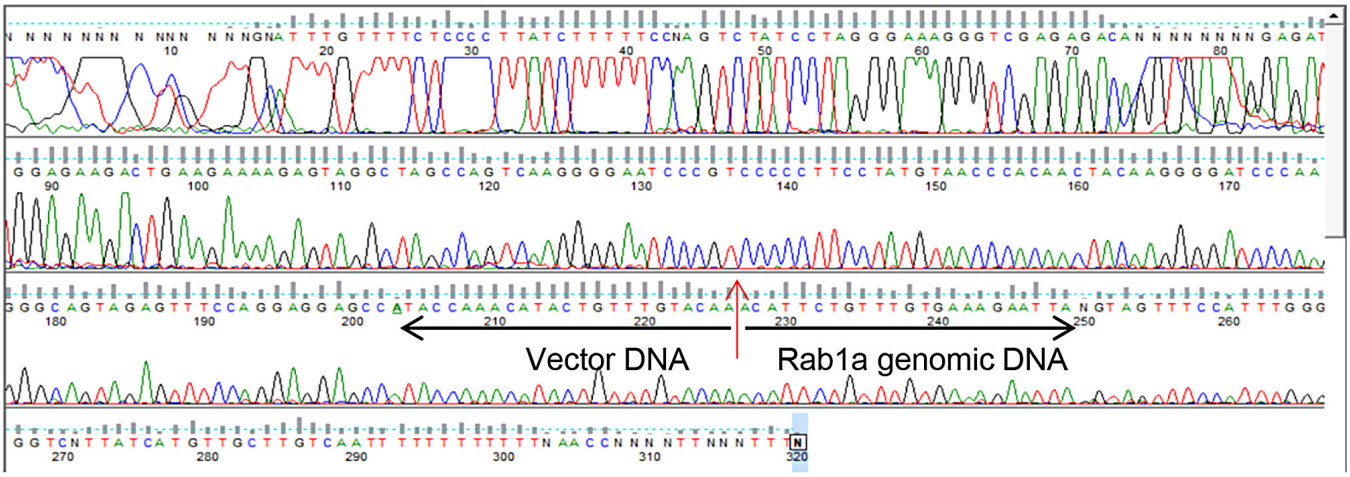

Figure 2. DNA sequence of the Rab1a insertion site. The nucleotide sequence near the splice junction joining the *Rab1a* exon 2 splice donor to the splice acceptor of the vector is indicated. The red arrow indicates the insertion site between *Rab1a* genomic DNA sequence and vector DNA sequence.

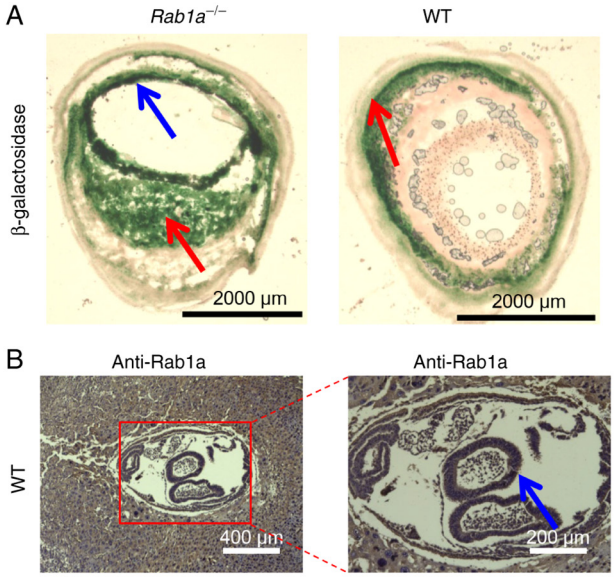

Figure 3. Expression of Rab1a in embryos. (A) X-gal staining of cryosections of Rab1a$^{-/-}$ KO and WT embryos. Corresponding WT sections served as negative controls for specific X-gal staining in Rab1a$^{-/-}$ knockout mice. (B) Immunohistochemical staining for the detection of Rab1a. Slices from WT embryos were stained with anti-Rab1a antibody and counterstained with hematoxylin. Tissue sections were stained with hematoxylin and eosin. The experiments shown in this figure were reproduced twice and representative images are shown. Scale bars: A, 2,000 μm; B, 400 μm. Higher magnification images are also shown in panel B (for higher magnification images scale bar, 200 μm). The blue arrows indicate positive staining. The red arrows indicate non-specific staining. X-gal, 5-bromo-4-chloro-3-indolyl β-D-galactopyranoside; WT, wild-type.

Chimeric male offspring were mated with WT C57Bl/6 mice to test for the germline transmission of the disrupted *Rab1a* allele. Heterozygous *Rab1a*$^{+/-}$ mice were viable and displayed no obvious abnormality in weight or fertility during a 12-month observation period (data not shown). To remove contaminating background heterozygosity, *Rab1a*$^{+/-}$ mice were backcrossed >10 generations with C57BL/6 mice.

Expression of Rab1a in mice. The expression of β-galactosidase is controlled by the endogenous *Rab1a* gene promoter. Thus, β-galactosidase expression was used in *Rab1a*$^{+/-}$ mice to document the pattern of Rab1a expression in mouse embryos. To visualize the expression pattern of *Rab1a*, X-gal staining of cryosections of *Rab1a*$^{+/+}$ and *Rab1a*$^{+/-}$ E7 embryos was performed; sections of WT embryos served as the negative controls. *Rab1a* was ubiquitously expressed in whole embryos (Fig. 3). To investigate endogenous Rab1a protein expression, WT E7 embryos were collected, sectioned and immunostained with anti-Rab1a antibodies. Similar to the *Rab1a* gene, Rab1a protein was ubiquitously expressed in the whole embryo (Fig. 3). Based on these findings, it was concluded that Rab1a protein expression was consistent with *Rab1a* β-galactosidase activity.

In addition, the expression of *Rab1a* during embryo development was examined using X-gal staining. At E15 embryo, *Rab1a* was mainly expressed in the intestine (Fig. 4) and a small amount of *Rab1a* was also detected in the brain (Fig. 4), as previously reported (28,29). In adult mice, *Rab1a* was expressed in the small intestine (Fig. 5).

Rab1a deficiency causes embryonic lethality. To generate *Rab1a*$^{-/-}$ mice, heterozygous *Rab1a*$^{+/-}$ mice were intercrossed. The genotypes of the offspring were identified at 2 weeks after birth. None of the 250 offspring were homozygous mutants (*Rab1a*$^{-/-}$) (total, 250; *Rab1a*$^{+/+}$, 94; *Rab1a*$^{+/-}$, 156; *Rab1a*$^{-/-}$, 0), and no increase in neonatal mortality was observed in the initial 2 weeks after birth. The ratio between the WT and heterozygote mice was 0.60, in accordance with Mendel's law. These results thus suggest that *Rab1a* is essential for embryonic development: one functional *Rab1a* allele is sufficient for murine embryonic development; however, a double mutant leads to embryonic lethality.

To characterize the effect of *Rab1a* mutation on embryonic development, timed matings (breeding we set up at 5 p.m. and the following morning the presence of a copulatory plug was examined at 7 a.m. If the presence of a copulatory plug was confirmed, this day was recorded as day 0.5) were performed between mice heterozygous for *Rab1a*. Embryos were collected at E12.5 and E14.5 from *Rab1a*$^{+/-}$ breeding mice and genotyped using PCR analysis with genomic DNA. No

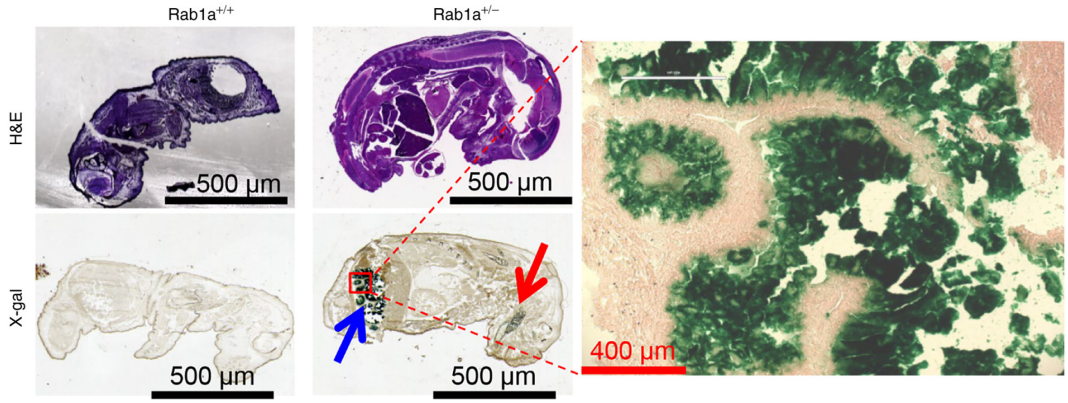

Figure 4. Expression of Rab1a in embryos at embryonic day 15. X-gal staining of cryosections of Rab1a$^{-/-}$ KO and WT embryos. Corresponding WT sections served as negative controls for specific X-gal staining in Rab1a$^{-/-}$ KO mice. Higher magnification images are also shown. The experiments in this figure were reproduced twice and representative images are shown. Scale bar, 500 μm; scale bar in higher magnification images, 400 μm. X-gal, 5-bromo-4-chloro-3-indolyl β-D-galactopyranoside; WT, wild-type; KO, knockout. The blue arrow indicates intestinal staining. The red arrow indicates brain staining.

Table I. Effects of Rab1a mutation on the number of viable embryos.

Stage	Total	Rab1a$^{+/+}$	Rab1a$^{+/-}$	Rab1a$^{-/-}$
E10.5	21	6	10	5
E11.5	23	9	14	0
E12.5	18	7	11	0
E14.5	15	5	10	0

E, embryonic day.

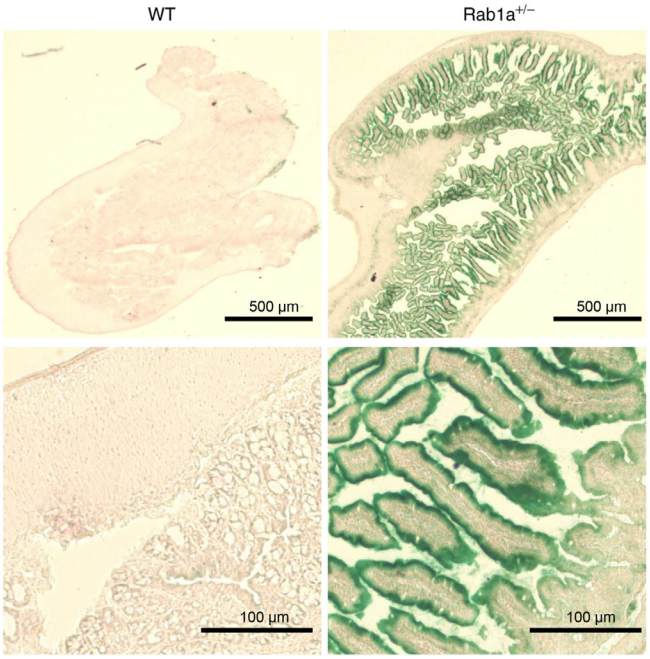

Figure 5. Expression of Rab1a in the small intestine of adult mice. X-gal staining of cryosections from the small intestine of Rab1a$^{-/-}$ KO and WT mice. Corresponding WT sections served as negative controls for specific X-gal staining in Rab1a$^{-/-}$ KO mice. Higher magnification images are also shown. Experiments in this figure were reproduced twice and representative images are shown (bottom panel). Scale bar, 500 μm; scale bar in higher magnification images, 100 μm. X-gal, 5-bromo-4-chloro-3-indolyl β-D-galactopyranoside; WT, wild-type; KO, knockout.

viable *Rab1a*$^{-/-}$ embryos were recovered (Fig. 6). The developmental retardation of *Rab1a*$^{-/-}$ embryos was apparent at E12.5, suggesting that embryonic lethality occurred prior to E12.5 (Fig. 6). Embryos at E10.5 and E11.5 were also collected and it was found that viable *Rab1a*$^{-/-}$ embryos were recovered at E10.5, whereas no viable *Rab1a*$^{-/-}$ embryos were recovered at E11.5; the data for viable embryos in different embryonic stages are summarized in Table I, the different numbers in the table indicate the viable embryos found in the different embryonic genotypes. Thus, *Rab1a* mutation-induced embryonic lethality occurred between E10.5 and E11.5.

Rab1a protein deficiency in Rab1a$^{-/-}$ *KO mice*. WT and mutant alleles were assessed using PCR of genomic DNA isolated from mice (Fig. 7A). Western blot analysis was also performed to test the successful disruption of the *Rab1a* gene in *Rab1a*$^{-/-}$ mice. E10.5 embryos were collected and genotyped using PCR. *Rab1a*$^{+/+}$ and *Rab1a*$^{-/-}$ embryos were lysed and used for western blot analysis with anti-Rab1a antibody. As shown in Fig. 7B, Rab1a was completely absent in *Rab1a*$^{-/-}$ embryos, indicating the functional loss of *Rab1a*; β-actin was used as a loading control.

One Rab1a allele is sufficient for resistance to LPS-induced sepsis. The loss of GDI2 in tumor cells alters the crosstalk between tumor cells and tumor-associated macrophages to enhance both local inflammation and tumor cell invasion and growth, resulting in inflammatory cytokine secretion by macrophages to promote metastatic growth (30). Moreover, Rab1a is required for NLRP3 inflammasome activation and inflammatory lung injury (31). Recently, the authors demonstrated that Rab1a bound to the ITIM domain of Siglec-G under normal homeostasis. By contrast, Rab1a was recruited to the ITIM domain during bacterial infection, suggesting that GDI2 and Rab1a may regulate immune response through interaction with the ITIM domain during bacterial infection (18). In the present study, to investigate whether Rab1a plays a role during bacterial infection, WT and *Rab1a*$^{+/-}$ mice were challenged

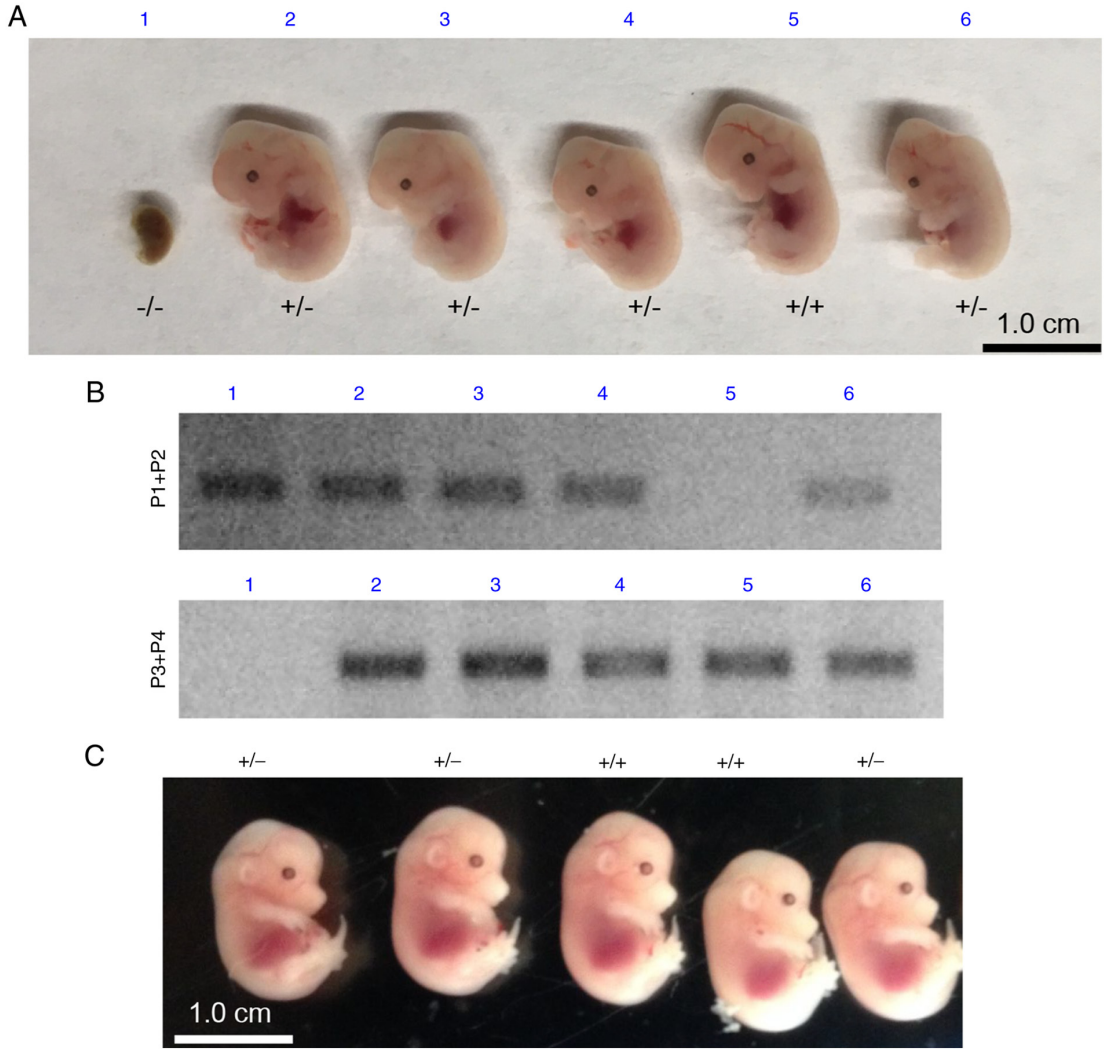

Figure 6. Rab1a mutant results in embryonic lethality. (A) Representative images of E12.5 embryos of the indicated genotypes. (B) Polymerase chain reaction genotyping results for the embryos in panel A using the indicated allele-specific primers. (C) Representative images of embryos at E14.5 of the indicated genotypes. Nos. 1-6 correspond to the same embryos in panels A and B. Scale bar, 1.0 cm. E12.5, embryonic day 12.5; E14.5, embryonic day 14.5.

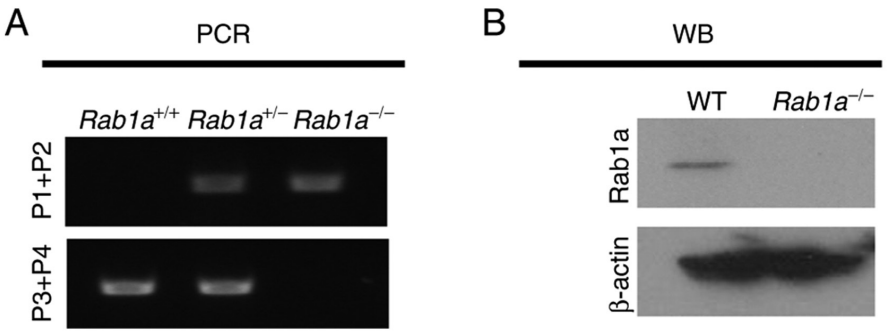

Figure 7. Analyses to demonstrate the deletion of the Rab1a gene. (A) Representative polymerase chain reaction results illustrating the mouse genotypes. (B) Loss of Rab1a in mice generated using the XB498 cell line. Proteins were extracted from embryonic tissues, separated by SDS/PAGE, and subjected to western blot analysis. The representative blots demonstrate the lack of Rab1a protein in embryo lysates of *Rab1a*$^{-/-}$ knockout mice in comparison to WT control mice. Actin levels were used as sample loading controls. Data are representative of two independent experiments. WT, wild-type.

with 10 mg/kg LPS and collected serum from the mice as previously described (21,22,24). As shown in Fig. 8, both WT and *Rab1a*$^{+/-}$ mice produced similar levels of inflammatory cytokines following LPS stimulation. Moreover, after 120 h, 50% (8/16, *Rab1a*$^{+/+}$) and 56% (9/16, *Rab1a*$^{+/-}$) of the mice did not survive; from data pooled from two independent experiments, a similar percentage of death was observed following LPS treatment (32) (data not shown); no significant differences were observed between the WT and *Rab1a*$^{+/-}$ mice as regards survival following the LPS challenge.

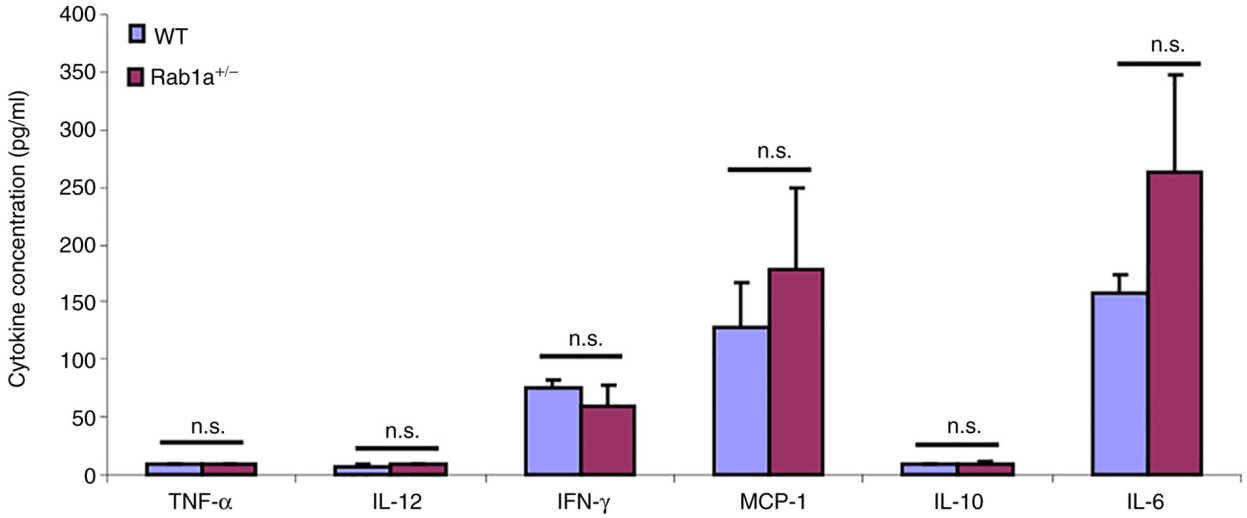

Figure 8. One Rab1a allele is sufficient for the resistance to LPS challenge. Serum concentrations of cytokines TNF-α, IL-6, IL-12, IL-10, MCP-1 and IFN-γ at 16 h following the lipopolysaccharide (LPS) challenge (mean ± SD, n=8) were measured by using a mouse cytokine bead array designed for inflammatory cytokines. The experiments in this figure were reproduced twice. n.s., no significant differences were found. TNF-α, tumor necrosis factor α; IL, interleukin; MCP-1, monocyte chemoattractant protein-1; IFN-γ, interferon γ.

Discussion

The transfer of material between organelles in eukaryotic cells is predominantly mediated by vesicular transport. GTP binding proteins play key roles in the regulation of vesicular traffic at several stages of the exocytic and endocytic transport pathways. Rab GTPases are small GTP-binding proteins in the Ras superfamily. Following a vesicle fusion event, Rab is returned to its membrane of origin by GDI. GDI proteins regulate the GDP-GTP exchange reaction of Rab family members that are involved in the vesicular trafficking of molecules between cellular organelles. GDIs decrease the rate of dissociation of GDP from Rab proteins and release GDP from membrane bound Rabs (1,33).

The authors have previously demonstrated that Rab1a may regulate the immune response through interaction with the ITIM domain during bacterial infection *in vitro* (18). To further investigate the function of Rab1a *in vivo*, the present study generated mice with a trapped *Rab1a* gene and uncovered a novel role for Rab1a during early embryonic development in mice. None of the 250 genotyped pups from *Rab1a* heterozygous mating pairs exhibited the homozygous deletion of the *Rab1a* allele. The present study was also unable to detect any viable *Rab1a* null embryos after E11.5, indicating a severe early embryonic defect caused by the complete loss of *Rab1a* function. However, one functional *Rab1a* allele is sufficient for murine embryo development, as the frequency of heterozygote offspring was as predicted.

Although Rab1a interacts with the ITIM domain during bacterial infection, there was no significant difference in cytokine production and survival between the WT and *Rab1a*$^{-/-}$ KO mice after the LPS challenge. These data suggest that one *Rab1a* allele is sufficient to maintain function. The conditional KO strategy is a useful method which may be used to solve the problem of embryonic lethality observed in conventional gene KOs (34). Therefore, to explore the function of Rab1a in hematopoietic cells in bacterial infection and to further investigate the role of Rab1a in embryonic development, a *Rab1a* conditional KO mouse model is needed (34).

Rab8 is reportedly necessary for the proper localization of apical proteins and the absorption and digestion of various nutrients in the small intestine (35). Previous research has indicated that Rab11a is essential for the proper localization of apical proteins in the intestine and that the loss of Rab11 leads to the mislocalization of apical proteins in the small intestine, as demonstrated using Rab11a intestine-specific knockout (IKO) mice (36). Rab25 KO mice exhibit increased numbers of intestinal neoplasms when crossed with APC$^{min/+}$ mice (37). With the use of X-gal staining, the present study found that Rab1a was mainly expressed in the small intestine in E15 embryos (Fig. 4) and in adult mice (Fig. 5). It would be of interest to determine whether Rab1a also plays an important role in controlling the proper localization of apical proteins or the absorption and digestion of various nutrients in the small intestine. However, intestine specific *Rab1a* conditional KO mice are required to further investigate the function of Rab1a in the small intestine.

Although the present study demonstrates that *Rab1a* is essential for embryonic development and homozygotes die between E10.5 and E11.5, the mechanisms underlying the regulatory effects of Rab1a on embryonic development remain unclear. Moreover, while it was found that Rab1a was mainly expressed in the small intestine in E15 embryos and in adult mice, it is not yet clear whether Rab1a plays a critical role in the small intestine. Further experiments using *Rab1a* conditional KO mice are thus required to provide further insight into this matter.

Acknowledgements

Not applicable.

Funding

The present study was supported by Grant R01AI137255 from the National Institutes of Health.

Availability of data and materials

The datasets used and/or analyzed during the current study are available from the corresponding author on reasonable request.

Authors' contributions

GYC designed the experiments. YW, DY and GYC conducted the experiments. GC wrote the manuscript. YW and GYC confirm the authenticity of all the raw data. All authors have read and approved the final manuscript.

Ethics approval and consent to participate

All procedures involving animals were approved by the University of Tennessee Health Science Center (UTHSC) Animal Care and Use Committee (IACUC), protocol nos. 17-117 (approved January 29, 2018) and 20-0211 (approved January 26, 2021).

Patient consent for publication

Not applicable.

Competing interests

The authors declare that they have no competing interests.

References

1. Pfeffer SR: Rab GTPases: Specifying and deciphering organelle identity and function. Trends Cell Biol 11: 487-491, 2001.
2. Zerial M and McBride H: Rab proteins as membrane organizers. Nat Rev Mol Cell Biol 2: 107-117, 2001.
3. Tisdale EJ, Bourne JR, Khosravi-Far R, Der CJ and Balch WE: GTP-binding mutants of rab1 and rab2 are potent inhibitors of vesicular transport from the endoplasmic reticulum to the Golgi complex. J Cell Biol 119: 749-761, 1992.
4. Nuoffer C, Davidson HW, Matteson J, Meinkoth J and Balch WE: A GDP-bound of rab1 inhibits protein export from the endoplasmic reticulum and transport between Golgi compartments. J Cell Biol 125: 225-237, 1994.
5. Zhuang X, Adipietro KA, Datta S, Northup JK and Ray K: Rab1 small GTP-binding protein regulates cell surface trafficking of the human calcium-sensing receptor. Endocrinology 151: 5114-5123, 2010.
6. Marie M, Dale HA, Sannerud R and Saraste J: The function of the intermediate compartment in pre-Golgi trafficking involves its stable connection with the centrosome. Mol Biol Cell 20: 4458-4470, 2009.
7. Wu G, Yussman MG, Barrett TJ, Hahn HS, Osinska H, Hilliard GM, Wang X, Toyokawa T, Yatani A, Lynch RA, *et al*: Increased myocardial Rab GTPase expression: A consequence and cause of cardiomyopathy. Circ Res 89: 1130-1137, 2001.
8. Machner MP and Isberg RR: A bifunctional bacterial protein links GDI displacement to Rab1 activation. Science 318: 974-977, 2007.
9. Neunuebel MR, Chen Y, Gaspar AH, Backlund PS Jr, Yergey A and Machner MP: De-AMPylation of the small GTPase Rab1 by the pathogen Legionella pneumophila. Science 333: 453-456, 2011.
10. Tan Y and Luo ZQ: Legionella pneumophila SidD is a deAMPylase that modifies Rab1. Nature 475: 506-509, 2011.
11. Sklan EH, Serrano RL, Einav S, Pfeffer SR, Lambright DG and Glenn JS: TBC1D20 is a Rab1 GTPase-activating protein that mediates hepatitis C virus replication. J Biol Chem 282: 36354-36361, 2007.
12. Zhang X, Wang X, Yuan Z, Radford SJ, Liu C, Libutti SK and Zheng XF: Amino acids-Rab1A-mTORC1 signaling controls whole-body glucose homeostasis. Cell Rep 34: 108830, 2021.
13. Thomas JD, Zhang YJ, Wei YH, Cho JH, Morris LE, Wang HY and Zheng XF: Rab1A is an mTORC1 activator and a colorectal oncogene. Cancer Cell 26: 754-769, 2014.
14. Xu BH, Li XX, Yang Y, Zhang MY, Rao HL, Wang HY and Zheng XF: Aberrant amino acid signaling promotes growth and metastasis of hepatocellular carcinomas through Rab1A-dependent activation of mTORC1 by Rab1A. Oncotarget 6: 20813-20828, 2015.
15. Xu H, Qian M, Zhao B, Wu C, Maskey N, Song H, Li D, Song J, Hua K and Fang L: Inhibition of RAB1A suppresses epithelial-mesenchymal transition and proliferation of triple-negative breast cancer cells. Oncol Rep 37: 1619-1626, 2017.
16. Takai Y, Sasaki T and Matozaki T: Small GTP-binding proteins. Physiol Rev 81: 153-208, 2001.
17. Fagerberg L, Hallström BM, Oksvold P, Kampf C, Djureinovic D, Odeberg J, Habuka M, Tahmasebpoor S, Danielsson A, Edlund K, *et al*: Analysis of the human tissue-specific expression by genome-wide integration of transcriptomics and antibody-based proteomics. Mol Cell Proteomics 13: 397-406, 2014.
18. Wu Y, Yang D and Chen GY: The role of the Siglec-G ITIM domain during bacterial infection. Cell Mol Biol 67: 163-169, 2021.
19. Chen GY, Muramatsu H, Kondo M, Kurosawa N, Miyake Y, Takeda N and Muramatsu T: Abnormalities caused by carbohydrate alterations in Ibeta6-N-acetylglucosaminyltransferase-deficient mice. Mol Cell Biol 25: 7828-7838, 2005.
20. Bundschu K, Knobeloch KP, Ullrich M, Schinke T, Amling M, Engelhardt CM, Renné T, Walter U and Schuh K: Gene disruption of Spred-2 causes dwarfism. J Biol Chem 280: 28572-28580, 2005.
21. Chen GY, Brown NK, Wu W, Khedri Z, Yu H, Chen X, van de Vlekkert D, D'Azzo A, Zheng P and Liu Y: Broad and direct interaction between TLR and Siglec families of pattern recognition receptors and its regulation by Neu1. Elife 3: e04066, 2014.
22. Wu Y, Yang D, Liu R, Wang L and Chen GY: Selective response to bacterial infection by regulating Siglec-E expression. iScience 23: 101473, 2020.
23. Chen GY, Chen X, King S, Cavassani KA, Cheng J, Zheng X, Cao H, Yu H, Qu J, Fang D, *et al*: Amelioration of sepsis by inhibiting sialidase-mediated disruption of the CD24-SiglecG interaction. Nat Biotechnol 29: 428-435, 2011.
24. Chen GY, Tang J, Zheng P and Liu Y: CD24 and Siglec-10 selectively repress tissue damage-induced immune responses. Science 323: 1722-1725, 2009.
25. Chen WV and Soriano P: Gene trap mutagenesis in embryonic stem cells. Methods Enzymol 365: 367-386, 2003.
26. Friedrich G and Soriano P: Insertional mutagenesis by retroviruses and promoter traps in embryonic stem cells. Methods Enzymol 225: 681-701, 1993.
27. Stryke D, Kawamoto M, Huang CC, Johns SJ, King LA, Harper CA, Meng EC, Lee RE, Yee A, L'Italien L, *et al*: BayGenomics: A resource of insertional mutations in mouse embryonic stem cells. Nucleic Acids Res 31: 278-281, 2003.
28. Ayala J, Olofsson B, Touchot N, Zahraoui A, Tavitian A and Prochiantz A: Developmental and regional expression of three new members of the ras-gene family in the mouse brain. J Neurosci Res 22: 384-389, 1989.
29. Olofsson B, Chardin P, Touchot N, Zahraoui A and Tavitian A: Expression of the ras-related ralA, rho12 and rab genes in adult mouse tissues. Oncogene 3: 231-234, 1988.
30. Said N, Sanchez-Carbayo M, Smith SC and Theodorescu D: RhoGDI2 suppresses lung metastasis in mice by reducing tumor versican expression and macrophage infiltration. J Clin Invest 122: 1503-1518, 2012.
31. Zhang Y, Wang L, Lv Y, Jiang C, Wu G, Dull RO, Minshall RD, Malik AB and Hu G: The GTPase Rab1 is required for NLRP3 inflammasome activation and inflammatory lung injury. J Immunol 202: 194-206, 2019.
32. Maitre B, Magnenat S, Heim V, Ravanat C, Evans RJ, de la Salle H, Gachet C and Hechler B: The P2X1 receptor is required for neutrophil extravasation during lipopolysaccharide-induced lethal endotoxemia in mice. J Immunol 194: 739-749, 2015.
33. Seabra MC and Wasmeier C: Controlling the location and activation of Rab GTPases. Curr Opin Cell Biol 16: 451-457, 2004.

34. Le Y and Sauer B: Conditional gene knockout using cre recombinase. Methods Mol Biol 136: 477-485, 2000.
35. Sato T, Mushiake S, Kato Y, Sato K, Sato M, Takeda N, Ozono K, Miki K, Kubo Y, Tsuji A, *et al*: The Rab8 GTPase regulates apical protein localization in intestinal cells. Nature 448: 366-369, 2007.
36. Sobajima T, Yoshimura S, Iwano T, Kunii M, Watanabe M, Atik N, Mushiake S, Morii E, Koyama Y, Miyoshi E and Harada A: Rab11a is required for apical protein localisation in the intestine. Biol Open 4: 86-94, 2014.
37. Nam KT, Lee HJ, Smith JJ, Lapierre LA, Kamath VP, Chen X, Aronow BJ, Yeatman TJ, Bhartur SG, Calhoun BC, *et al*: Loss of Rab25 promotes the development of intestinal neoplasia in mice and is associated with human colorectal adenocarcinomas. J Clin Invest 120: 840-849, 2010.